Back propagation modelling of shear stress and viscosity of aqueous Ionic-MXene nanofluids

Asif Afzal[1*], Yashawantha K. M. [2], Navid Aslfattahi[3, 4], R Saidur[3, 6*], Abdul Razak R. K[1], Ram Subbiah[7]

[1]Mechanical Engineering, P. A. College of Engineering (Affiliated to Visvesvaraya Technological University, Belagavi), Mangalore-574153, India
[2]Department of Chemical Engineering, National Institute of Technology, Warangal- 506004, Telangana
[3] Research Center for Nano-Materials and Energy Technology (RCNMET), School of Science and Technology,
[4]Sunway University, Bandar Sunway, Petaling Jaya, 47500, Selangor Darul Ehsan, Malaysia
[5]Department of Mechanical Engineering, Faculty of Engineering, University of Malaya, 50603, Kuala Lumpur
[6]Department of Engineering, Lancaster University, Lancaster, LA1 4YW, UK
[7]Gokaraju Rangaraju Institute of Engineering & Technology, Hyderabad, India

*Corresponding author: asif.afzal86@gmail.com, saidur@sunway.edu.my

Abstract

Back-propagation modelling of viscosity and shear stress of Ionic-MXene nanofluid is carried out in this work. The data for Ionic-MXene nanofluid of 0.05, 0.1, and 0.2 weight concentration (wt. %) is collected from the experimental analysis. Shear stress and viscosity as a function of shear rate and wt. % of MXene nanoparticles is used as input. Additionally, viscosity as a function of temperature and % of MXene nanoparticles is collected separately. Based on the possible combinations five back-propagation algorithms (BPA) are developed. In each algorithm five models depending upon the number of neurons in the hidden layer are used. The training and testing of all the model in each algorithm is performed. Statistical analysis of the network output is done to evaluate the accuracy of models. Model 1 is found to have lower accuracy than the remaining models. The training and testing is of the algorithms is satisfactory as the network output is found to be in comfortably good agreement with the desired experimental output.

Keywords: Neural networks; shear stress; viscosity; MXene; nanofluids; algorithms.

Nomenclature

ANN	Artificial neural network
MSE	Mean square error
RMSE	Root mean square error
BPA	Back propagation algorithm
RBF	Radial basis function
MLP	Multilayer perceptron
wt%	Weight concentration

1. Introduction

The development of industries has given extreme importance in expanding the performance of the heat transfer equipment by adopting various methods. Several methods have been adopted to increase the performance of the heat transfer system by enhancing the heat transfer rate. However, increased surface area and flow arrangement with different design may increase the performance. This may lead to complications in the manufacturing of such designs. Therefore, enhancing the thermo physical properties of base fluids have attracted various researchers due to the possibilities of maintaining the compactness of the heat transfer system. It is well known that fluids such as Water, Ethylene glycol (EG), EG and water mixture, Propylene glycols (PEG), PEG and water mixtures and oils are generally considered as the base fluid as they possess good heat transfer properties and can be used at numerous operating temperatures. Thermo physical properties of these fluids can be improved by introducing nano-sized solid particles into it. These nano-sized particles are generally known as nanoparticles, and the fluids containing these nanoparticles are termed as nanofluids. Nanofluids have shown better thermo physical properties than their respective base fluids. However, the enhanced thermal conductivity when nanoparticles dispersed into the base fluid has attracted the attention of researchers [1].

Many researchers studies have proven enhanced thermal conductivity when nanoparticles of different materials are used [2,3]. Subsequently, heat transfer studies have depicted with an enhanced heat transfer coefficient [4–6]. The studies related to the effective use of these nanofluids in applications such as solar collectors [7,8], refrigeration [9,10], heat pipes [11,12], nuclear reactors [13], automobile industry [14] have shown significant improvement in their performance. Thermo physical properties of nanofluids have shown variation depends upon the various factors such as nanoparticle material, particle concentration, nanoparticles size and shape and temperature [15]. Other factors such as the effect of ultrasonication time and surfactant have shown a significant effect on thermo physical properties [16–20]. The significant effect on thermal conductivity is widely reported considering nanoparticle concentration and temperature [21]. Results indicate that increasing concentration and temperature increases the thermal conductivity [22]. Viscosity is one of the essential property which is used for analysis in heat transfer. The viscosity of nanofluids increases with an increase in nanoparticle concentrations and diminishes as the temperature increases [23]. Yashawantha et al., [24] performed the viscosity measurement considering the graphite nanoparticles dispersed in EG. The study showed that viscosity depends on concentration and temperature. Subsequently, correlations were developed to predict the viscosity of EG-Graphite nanofluid.

The process of determining the thermo physical properties of nanofluids experimentally consumes more time compared to the numerical method used for the heat transfer study [25]. However, to perform heat transfer studies numerically [26], the properties of these nanofluids are to be determined experimentally as no numerical approaches are available to estimate these properties. Moreover, the addition of nanoparticles into base fluid increases the thermal conductivity and at the same time viscosity also increases. Pumping power increases [27] as a result of increased viscosity and also it reduces the convective heat transfer coefficient [28]. Therefore, an experimental investigation is necessary to find the viscosity of the nanofluid. However, researchers have developed correlations and modelling to reduce the number of experiments required to find these properties. Such modelling approach is accountable for the accurate prediction of thermo physical properties [29]. Machine learning model such as artificial neural network (ANN), Radial Basis Function (RBF), multivariable polynomial regression (MPR) and multivariate adaptive regression splines (MARS) are the tool used for the prediction of thermo physical properties of nanofluids.

Esfe et al., [30] performed ANN modelling for evaluation of viscosity of water - TiO_2 nanofluid considering temperature and mass concentration as an input variable. They achieved a regression coefficient of 0.9998 when ANN model was structured with a single hidden layer with 4 neurons. Afrand et al., [31] presented optimum predicting model (ANN) for relative viscosity of multi-walled carbon nanotubes dispersed in water considering their experimental data. Vakili et al., [32] performed a hybrid model (genetic algorithm (GA) and artificial neural network) to predict the viscosity of graphene nanoplatelets – deionized water (DI) nanofluids. Experimental results obtained for these nanofluids considered as target, temperature and nanoparticles concentration were considered for input to perform this predictive analysis. Amani et al., [33] studied the ANN and GA approach in predicting the thermal conductivity and viscosity of water based spinel - $MnFe_2O_4$ nanofluid considering the input variables as magnetic field, concentration and temperature. Their study was conducted under multiobjective optimization (thermal conductivity and viscosity) considering three different algorithms (Levenberg-Marquardt, quasi-Newton and resilient back propagation) approach to training the data. Zhao Liu [34] constructed an RBF neural network to predict the thermal conductivity and viscosity of water - Al_2O_3 nanofluids taking nanoparticle concentration and temperature as an input variable. The comparative analysis made with RBF neural network and experimental results have showed excellent ability of RBF network to predict the thermal conductivity and viscosity of Al_2O_3 - water. Similar kind of study was conducted by Derakhshanfard and Mehralizadeh [35] considering RBF method of ANN modelling to predict the viscosity of crude-oil based nanofluids (NiO, WO_3, TiO_2, ZnO and FeO_3). They have considered temperature and nanoparticle concentration as the input variables.

Shadloo et al., [36] performed ANN modeling to predict pressure drop in two-phase flow in horizontal long pipes for wide range of operating condition considering the pipe diameters, and fluid characteristics. Predicted data of pressure drop showed with good accuracy (deviation less than 5%). Ansari et al., [37] reported comprehensive study on modelling viscosity of nanofluids using feed-forward back-propagation neural networks considering 1620 experimental data points from literature. They have considered different training algorithm such as Scaled Conjugate Gradient (SCG), Levenberg-Marquardt (LM), Bayesian Regulation back propagation (BR), and Resilient back Propagation (RP). Their study investigated effect on network precision for the different transfer functions (Radial basis (radbas), Tan-sigmoid (tansig), Log-sigmoid (logsig), Hard-limit (hardlim), Triangular basis (tribas) and Soft max transfer function (softmax)) in hidden layer. The input parameter such as temperature, nanoparticle size, shear rate, density of nanoparticles and concentration were taken to develop a neural network. The neural network comprising LM training model with 1 hidden layer and 23 neurons with tan-sigmoid and purelin transfer functions in the hidden and output layers was found to deliver the best performance compared to others.

Ahmadi et al., [38] presented three different algorithm (ANN-MLP, MARS and MPR) to predict the viscosity of Silver/water nanofluid choosing experimental results reported from the literature. The input variables selected in the modelling process are the size of nanoparticles, temperature and concentration of the silver nanoparticles. Naik and Vinod [39] implemented the Feed forward ANN with Levenberg-Marquardt algorithm approach for predicting the apparent viscosity of carboxymethyl cellulose (CMC) based Fe_2O_3, Al_2O_3 and CuO nanofluids. The results of experimentally obtained apparent viscosity was considered as target for training the neural network. Prediction obtained from the ANN modelling showed good agreement with experimental results. Shahsavar et al., [40] implemented the ANN model to predict the thermal conductivity and viscosity of paraffin - Al_2O_3 nanofluid using their experimental data. Multiple Inputs (shear rate, nanoparticles concentration, and temperature) were considered for modelling the viscosity of paraffin - Al_2O_3 nanofluid.

To obtain a precise model to predict the viscosity of SiO_2/EG- water nanofluids, Ahmadi et al., [41] employed MLP and RBF algorithms to test the experimental data. For this analysis experimental data was collected from the literature and the accuracy of the proposed model was validated through performing error analysis. Toghraie et al., [42] experimentally investigated the dynamic viscosity of Silver/Ethylene glycol nanofluid by varying temperature and volume fraction. They designed the best architecture of the ANN model to predict the dynamic viscosity of this nanofluid.

A unique multilayer perceptron model was developed by Yadav et al., [43] to estimate the viscosity of EG based Al_2O_3, CeO_2, and CuO nanofluids from their experimental results. The proposed structure of the neural network shows a fair agreement in predicting the viscosity results when compared on experimental data. Parashar et al., [44] developed ANN modelling for viscosity

(377 data) of EG based nanofluids considering the literature data. They have considered the diameter of the nanoparticles, temperature, and nanoparticle concentration as inputs variables and effective dynamic viscosity (μ_{nf}/μ_{bf}) as a target. Optimum model (2 hidden layers and 45 neurons in both the hidden layers) was obtained with performing modelling with varying different set of neurons in the hidden layer. The comparison made with experimental results and predictive results obtained from ANN showed an accurate prediction of effective dynamic viscosity of EG based nanofluids.

Alade et al., [45] presented a comparison study considering ANN and Bayesian support vector regression (BSVR) model for predicting the relative viscosity of nanofluids. For this purpose 19 different nanofluids results (1425 experimental data) from the literature were considered. To determine the optimum structure of model volume concentration, density of nanoparticles, fluid temperature, size of nanoparticles, and viscosity of base fluids were considered as input parameter. The results obtained from optimized BSVR model based on all possible input combinations were compared with the ANN model consisting of best model at two hidden layers with 10 neurons per hidden layer. The results indicated that the BSVR model exhibits superior prediction results compared to the ANN model and existing empirical model.

Parashar et al., [46] investigated viscosity of MXene nanomaterials-palm oil nanofluids experimentally, subsequently to predict the viscosity results ANN modelling approach was used. Temperature and nanoflakes concentration were considered as inputs to the ANN model, whereas dynamic viscosity was the output of the model. The prediction obtained from ANN modelling was in excellent agreement with the experimental data. The modeling work related to viscosity of nanofluids presented in literatures have showed very good prediction of data with multiple input variable compared to conventional method (correlation). However, most of studies have considered to predict the viscosity using different algorithm. Whereas, shear stress modelling of such nanofluids are not reported. Moreover, the shear stress is an important parameter in fluid flow and heat transfer. In this article the different back propagation modelling algorithms for shear stress and viscosity as a function of shear rate and MXene nanoparticle concentration in aqueous Ionic fluid is carried out. Five back propagation algorithms are developed for the modeling and prediction of viscosity and shear stress.

2. Data collection and Back propagation algorithms (BPA)

2.1 Data collection

Nanofluid of aqueous Ionic-MXene is prepared using Ionic liquid (1,3-Dimethylimidazolium dimethyl-phosphate). MXene nanoparticles of weight concentration (wt. %) 0.05, 0.1, and 0.2 are dispersed in the Ionic solution. MXene were initially synthesized using the MAX phase material. Magnetic stirring and probe sonication of the synthesized MXene nanoparticles in Ionic solution was followed to obtain the nanofluid. For further details of synthesizing of nanoparticles and preparation of nanofluid can be referred in [47]. Thorough characterization of the obtained MXene-Ionic nanofluid is performed in the reported work [47]. This experimental work performed is further used for the regression of the data using back-propagation algorithm. The data to perform the back-propagation modelling of shear stress and viscosity is taken from the same experimental work [47].

2.2 Back propagation modelling

The back propagation ANN (artificial neural networks) is a multi-layered FF (feed forward) network, and is the most popularly used. It is also one of the most basic and most popular methods of supervised neural network training. The back-propagation operates by changing and adjusting the non-linear relation between input and output. In general, two phases are the training & testing of the back propagation network. The network is feed with inputs and the appropriate classifications during the training process. For example, an encoded image of a face can be the input and the output can be described by a code which corresponds to the person's name [48–51].

In Figure 1 the BPA developed for the present work is shown. It should be noted that in BPA developed for regression modelling of shear stress and viscosity the inputs are 1) shear rate, 2) nanoparticle wt. % in Ionic solution, and 3) temperature. Based on the combinations the BPA are totally 5 in number. The combinations of the proposed BPA with input and output are mentioned in Table 1. These BPA proposed are based on the given number of inputs and outputs obtained experimentally. Algorithm 1 and 4 and algorithm 2, 5 have same outputs but with different methods. In Algorithm 1 or 2 which is actually same gives only one output at a time. Hence to differentiate this the BPA is designated as Algorithm 1 if the output is viscosity and as

Algorithm 2 when the output is shear stress. However, Algorithm 4 or 5 gives two outputs at a time. When viscosity is used from the BPA, it is called as Algorithm 4 and when shear stress is used it is mentioned as Algorithm 5. This naming convention is followed to avoid confusion in the statistical analysis of the data predicted for training and testing.

In each Algorithm the regression is performed varying the number of neurons in the hidden layer. In Table 2 the naming convention followed for each model in every BPA is provided. Model 1 to Model 5 is general name designated for BPA having neurons 1 to 5 respectively. The model pattern in the form Model A-B-C represents BPA model with A as number of inputs, B as number of neurons in hidden layer, and C as outputs. For example Model 2-1-2 represents BPA having 2 inputs, 1 neuron in hidden layer, and 2 outputs. This convention is followed for the analysis of training and testing results obtained.

Table 1. Algorithms developed based on input and output combinations

Algorithm no.	Inputs	Output	Output neurons
Algorithm 1	Shear rate & wt. %	Viscosity	1
Algorithm 2	Shear rate & wt. %	Shear stress	1
Algorithm 3	Temperature & wt. %	Viscosity	1
Algorithm 4	Shear rate & wt. %	Viscosity	2
Algorithm 5	Shear rate & wt. %	Shear stress	2

Table 2. Model names followed in the proposed BPA

<table>
<tr><th>Algorithm no.</th><th>Model no.</th><th>Model pattern</th><th>Neurons in input layer</th><th>Neurons in hidden layer</th><th>Neurons in output layer</th></tr>
<tr><td rowspan="5">Algorithm 1, 2, and 3</td><td>Model 1</td><td>Model 2-1-1</td><td>2</td><td>1</td><td>1</td></tr>
<tr><td>Model 2</td><td>Model 2-2-1</td><td>2</td><td>2</td><td>1</td></tr>
<tr><td>Model 3</td><td>Model 2-3-1</td><td>2</td><td>3</td><td>1</td></tr>
<tr><td>Model 4</td><td>Model 2-4-1</td><td>2</td><td>4</td><td>1</td></tr>
<tr><td>Model 5</td><td>Model 2-5-1</td><td>2</td><td>5</td><td>1</td></tr>
<tr><td rowspan="3">Algorithm 4 and 5</td><td>Model 1</td><td>Model 2-1-2</td><td>2</td><td>1</td><td>2</td></tr>
<tr><td>Model 2</td><td>Model 2-2-2</td><td>2</td><td>2</td><td>2</td></tr>
<tr><td>Model 3</td><td>Model 2-3-2</td><td>2</td><td>3</td><td>2</td></tr>
</table>

	Model 4	Model 2-4-2	2	4	2
	Model 5	Model 2-5-2	2	5	2

2.3 Statistical analysis

For the developed BPA the statistical analysis is performed to know their performance. %AAD (error deviation %), error of mean square (MSE), *R* (correlation coefficient), and RMSE (root mean square error) are employed for the BPA accuracy evaluation. Equations 1-4 are adopted for the estimation of these parameters.

$$\%AAD = \frac{1}{\mathrm{P}}\left(\sum_{a=1}^{P}\left|\frac{V_{DO}-V_{NO}}{V_{DO}}\right|\right)100 \tag{1}$$

$$MSE = \frac{1}{\mathrm{P}}\left(\sum_{a=1}^{P}(V_{DO}-V_{NO})^2\right) \tag{2}$$

$$RMSE = \sqrt{\frac{1}{\mathrm{P}}\left(\sum_{a=1}^{P}(V_{DO}-V_{NO})^2\right)} \tag{3}$$

$$R = \sqrt{1-\frac{\sum_{a=1}^{P}(V_{DO}-V_{NO})^2}{\sum_{a=1}^{P}(V_{DO(mean)}-V_{NO})^2}} \tag{4}$$

In the above equations P is the number of data points, V_{DO} and V_{NO} represents the desired output obtained experimentally and network output obtained from BPA respectively. In statistical analysis the lower %AAD value dictates the accuracy. The *R* value should be high enough to represent better accurate model which can go up to max equal to 1. MSE and RMSE of the model should be low enough (as low as possible) to show that the model is more accurate.

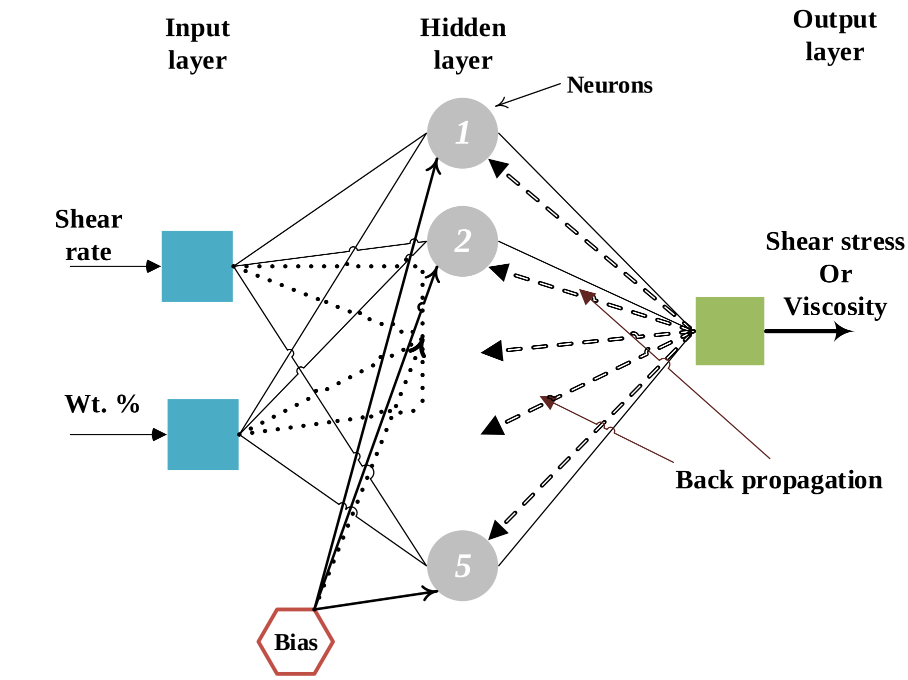

(a) Algorithm 1 and 2

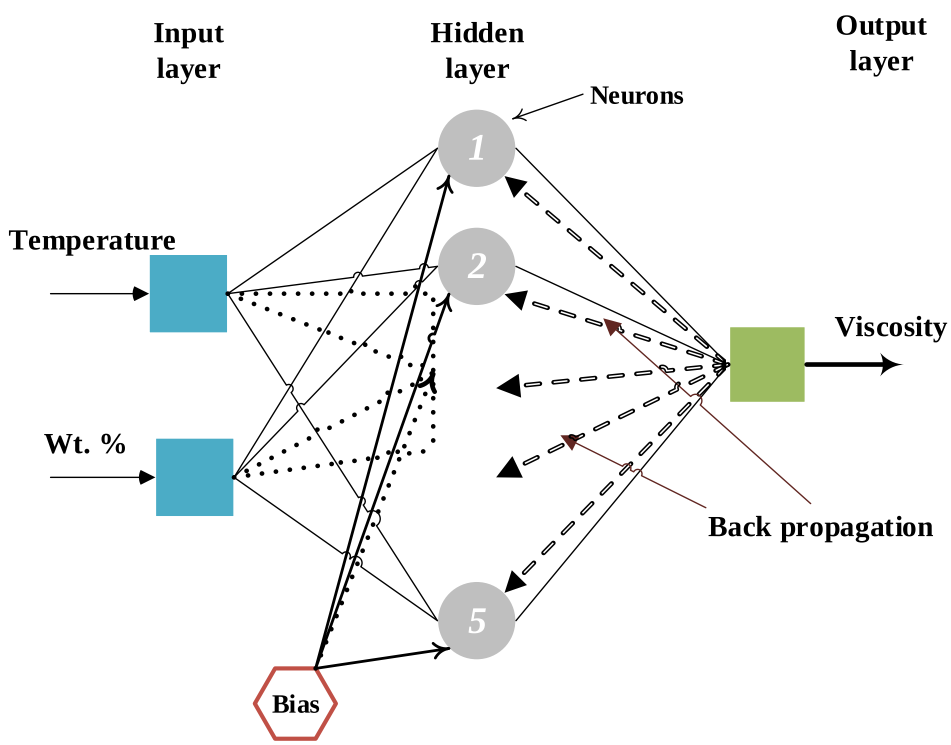

(b) Algorithm 3

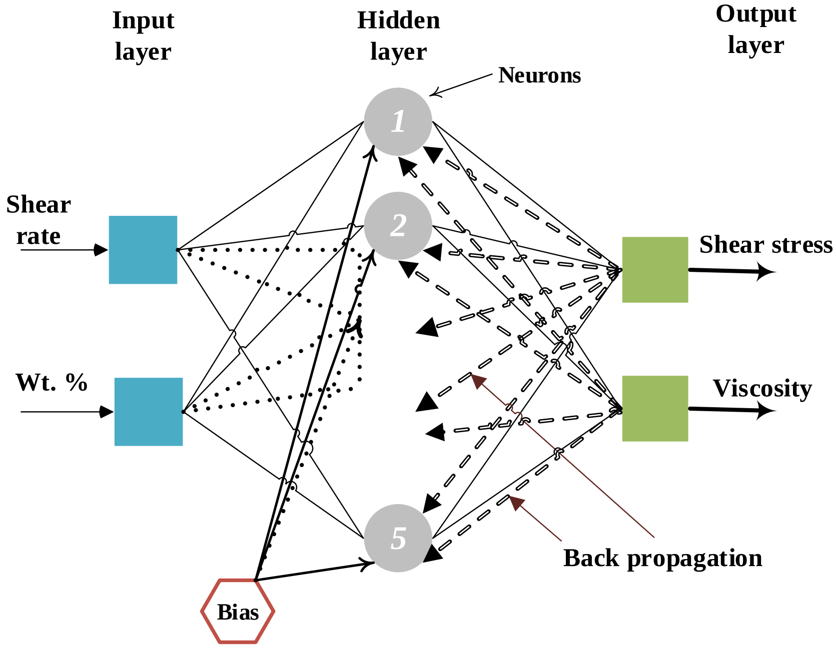

(c) Algorithm 4 and 5

Figure 1. Back propagation algorithms (BPA) developed for modelling of shear stress and viscosity individually (Algorithm 1, 2, and 3) and combined (Algorithm 4 and 5). Algorithm 1, 2 and Algorithm 4, 5 are same as the input for them is same i.e. shear rate and nanoparticle wt. %.

3. Results and discussion

The back propagation modelling of shear stress and viscosity as a function of shear rate and MXene nanoparticle wt. % in aqueous Ionic solution is analyzed in this section. Initially, the statistical analysis of BPAs is performed and then the predictions from the network during training and testing is presented. The prediction by different BPA using 5 models is discussed separately.

In Figure 2 the MSE of BPA 1 to 5 is shown for models 1 to 5 obtained from the training and testing of the network. Each model represents the number of neurons in the hidden layer. The BPA represents the parameter modelled like shear stress or viscosity. From the results it can be seen that the MSE highest is for BPA 5 at Model 1. Further observation reveals that for Model 1 in all BPA the MSE is comparatively higher. The reason is the single neuron in the hidden layer which finds difficult to adjust its weight to the fluctuating data with respect to inputs. The back propagation of error with single neuron is a difficult task to get the desired output. Therefore the network output with single neuron (Model 1 or Model A-1-C) will usually have large error than the other models. For BPA 5 the error is highest because the outputs involved in this algorithm are two which are shear stress and viscosity combined. In testing of the network the MSE is frequent than the training network. The MSE involved in training and testing is nearly same.

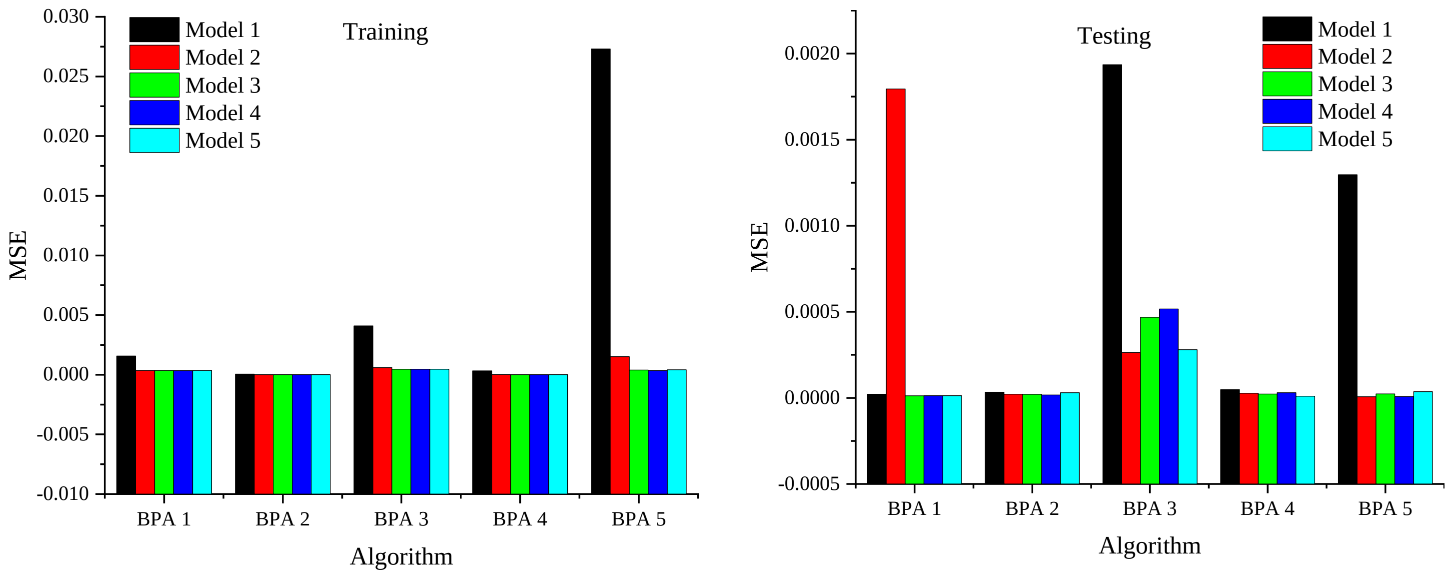

Figure 2. MSE of all the algorithms and models

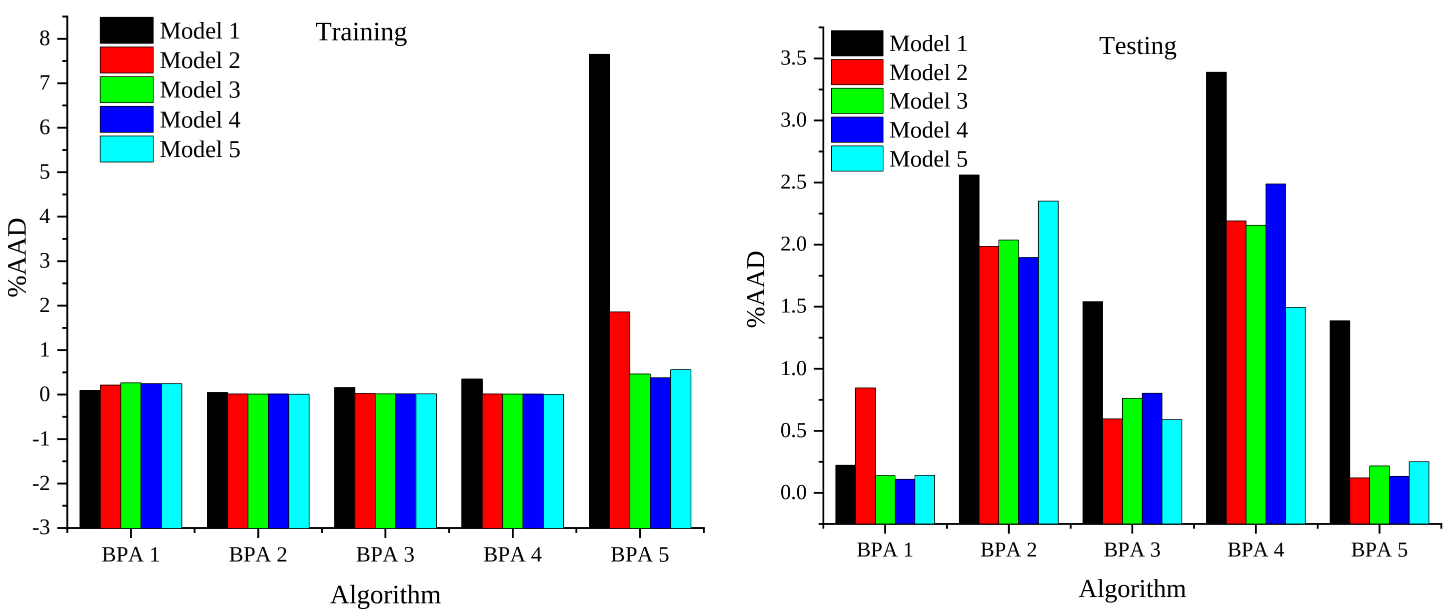

Figure 3. Error deviation by each algorithm and model

From Figure 3 the error deviation is shown for all the models and algorithms. In the training part the %AAD of each model is very close to 0 showing a greater fitness of the models in prediction of the output, except at BPA 5 the model 1 has shown more deviations. In the testing part of the network, BPA 1 model 2 has shown slightly more %AAD than the models. In rest of the algorithms model 1 is having more %AAD. In testing of the data obtained by network the %AAD indicates some instability of model. However BPA 5 provides %AAD very close to 0 for models 2 to 5.

The RMSE value for all models is shown in Figure 4. The error is less than 0.08 for all models in each algorithm. For most of the models the RMSE is very close to 0.01 indicating that the predicted values are close to desired values. BPA 1 for all models has shown the lowest error and BPA 5 is also predicted sufficiently the output as the error is low. The error developed by the model 1 in each algorithm is again clearly noticeable. The correlation coefficient must be very close to 1 indicating the model accuracy. In Figure 5 the R value is shown for each model. The R indicates that the training of the BPA is successful as it value is very close to 1. Only model 1 in each BPA is having slightly lower R value while other models are suitable. In training for model 2 to 5 in each training algorithm the R is closer to 1 i.e. 0.99. Model 5 having 5 neurons in hidden layer has provided the most accurate model in all aspects. The MSE, %AAD, RMSE, and R value of model 5 is better than the other models in each algorithm.

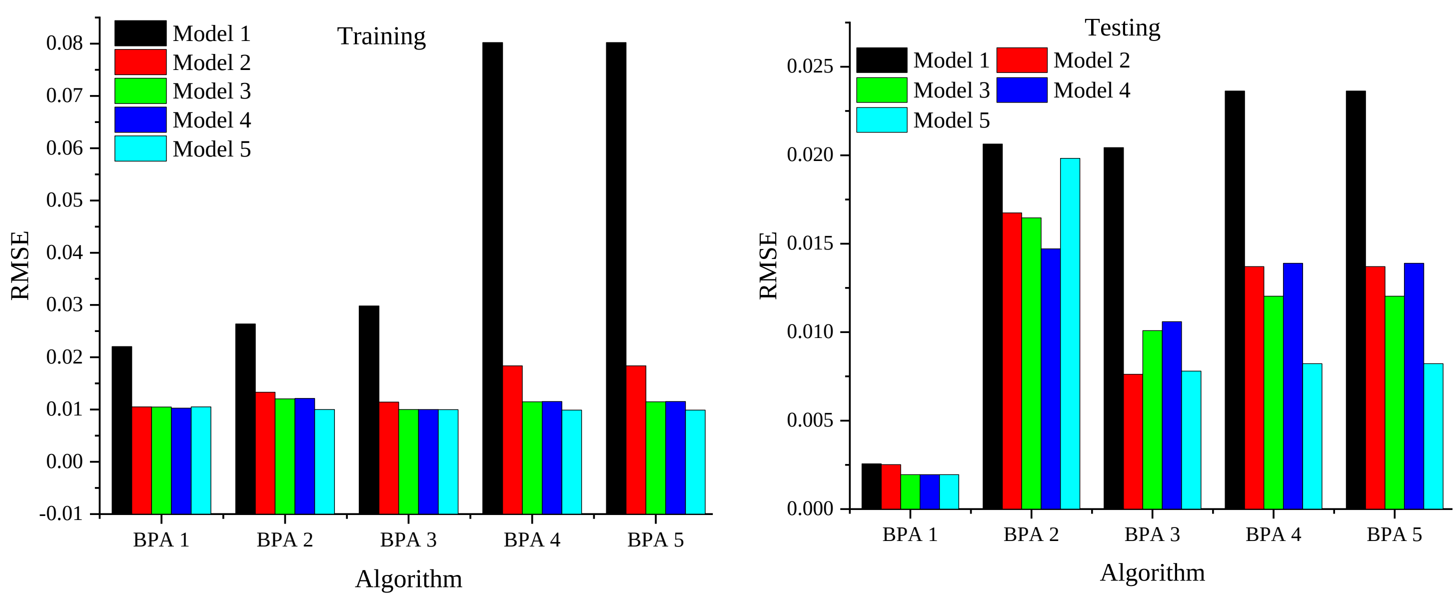

Figure 4. RMSE between the desired and network output

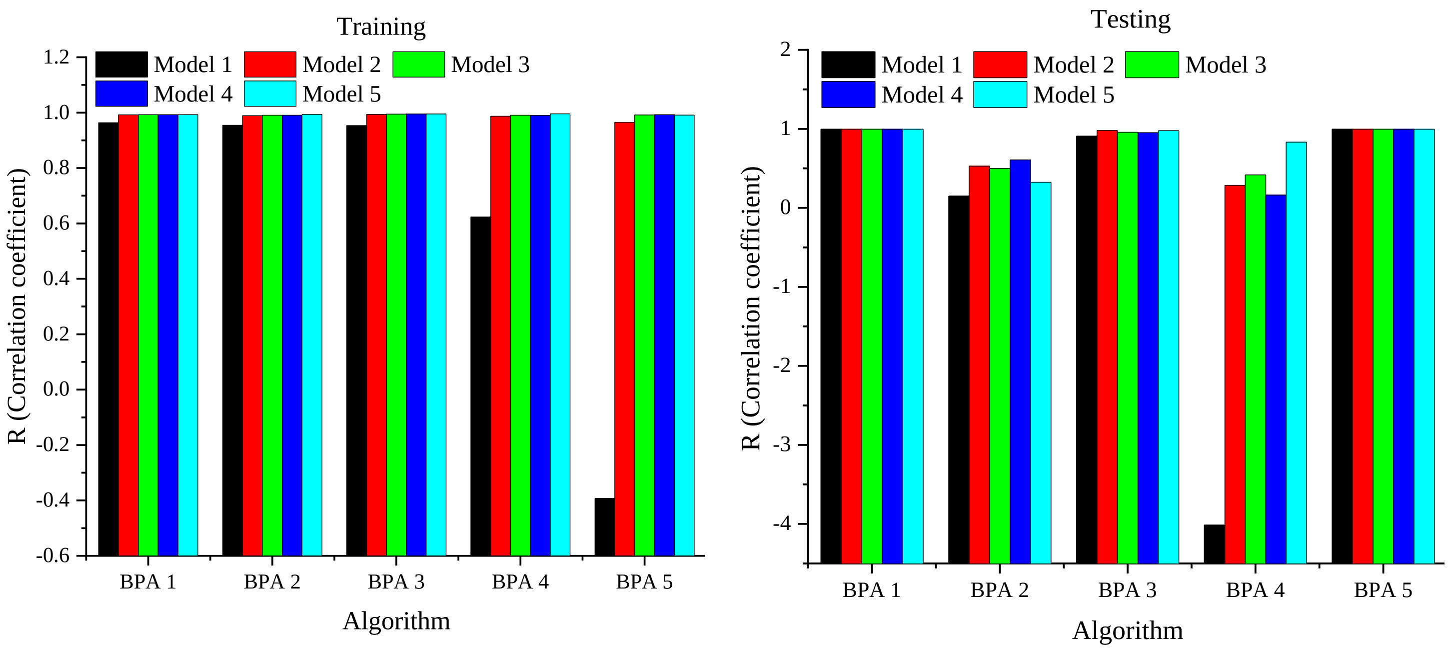

Figure 5. Correlation coefficient obtained from 5 models and 5 BPAs

In Figure 6 the viscosity predictions by the BPA 1 is provided for training data set. The data set is 400 points long for training and 30 points long in testing. For each model the training data set allotted is maximum to get the predictions properly. Testing is carried to know how well the network predicts after successful training of the model. In Figure 6 (a) the training results as obtained by the algorithm BPA 1 is shown. The viscosity predictions with shear rate and MXene wt. % is input. The model 2-1-1 to model 2-5-1 predictions are shown in the figure. The experimental results and the BPA 1 results by each model are of same trend. However except model 2-1-1 the predictions by BPA 1 is very close to the experimental results. The inset figure clearly indicates which model is most close to the desired output. Model 2-5-1 is very close the experimental readings indicating successful training. In Figure 6 (b) the testing predictions by the BPA 1 after training is shown. All model are here showing a good match with the experimental readings. Hence it can be said that BPA 1 and models 2 to 5 are good in predicting the viscosity of MXene-Ionic nanofluids.

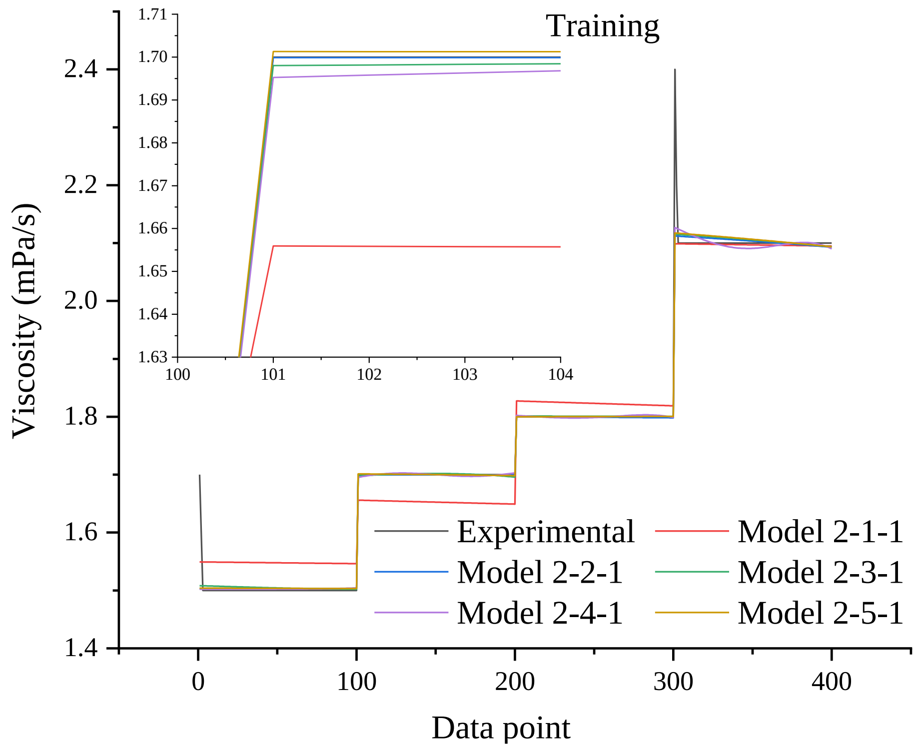

(a) Prediction by BPA 1 and experimental values

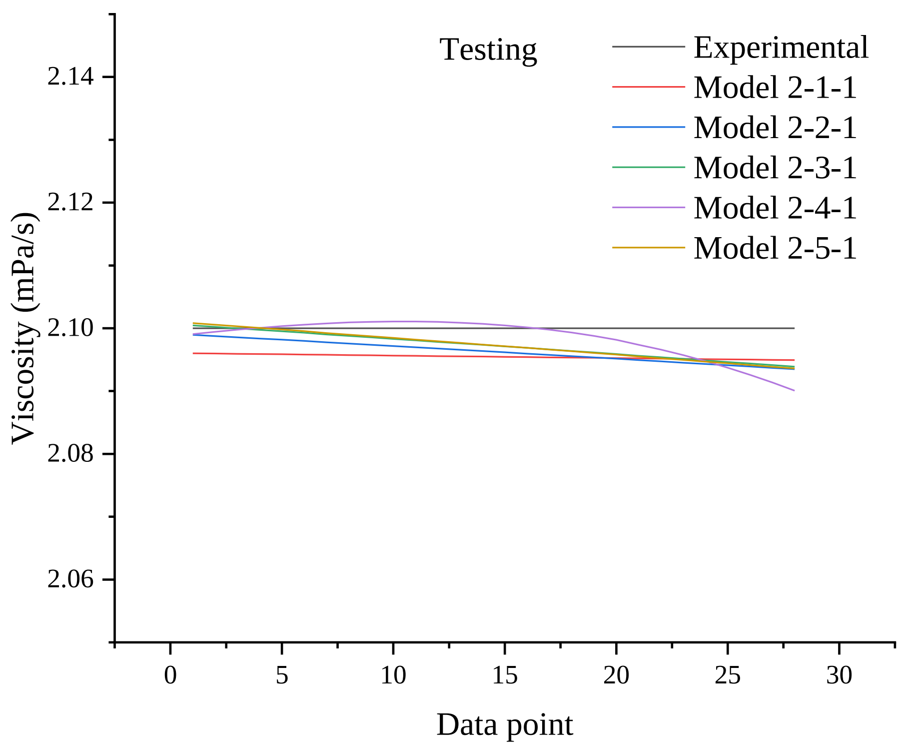

(b) Prediction by BPA 1 and experimental values

Figure 6. Training/testing results by BPA 1

Figure 7 shows the training of the BPA 2 by 5 models to predict the shear stress having same input as BPA 1. It is worth observing that with the increase of neurons in the hidden layer the prediction i.e. training of the BPA 2 becomes more fit. The R-squared value is mentioned at the bottom left corner to show how close the experimental values and network values are. If R-squared value is close to unity, it indicates the model predicts the output more accurately. Model 3, 4, and 5 having R-squared 0.99 showing a good fit between experimental and BPA 2 values. The deviations by model 1 and model 2 are very clear as the R-squared value is slightly more than 0.95. Model 3 to model 5 are successfully trained and are fit for predictions. Further in Figure 7 it should be noted that for model 5 the fitness of data is highest showing that 5 neurons are suitbale for the data more appropriately. The basic reason can be attributed to the back propagation of error to a greater number of neurons which can make the weight and bias values adjustment acordingly. For lower neurons the error corrections is having less scope so the dispute with the experimental observations.

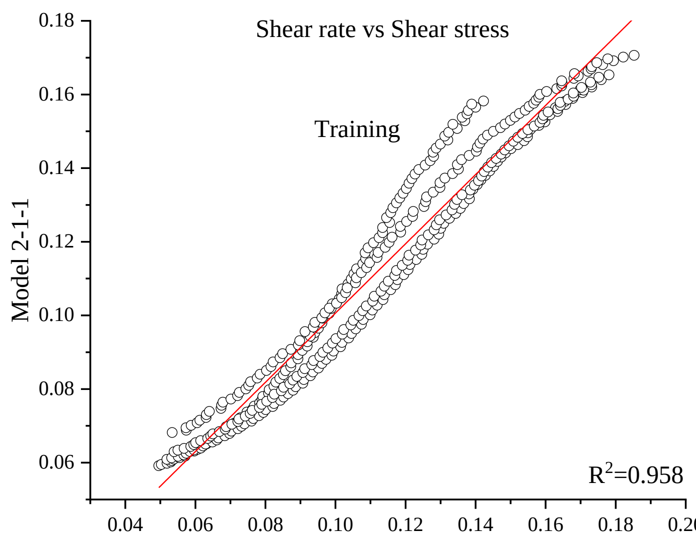

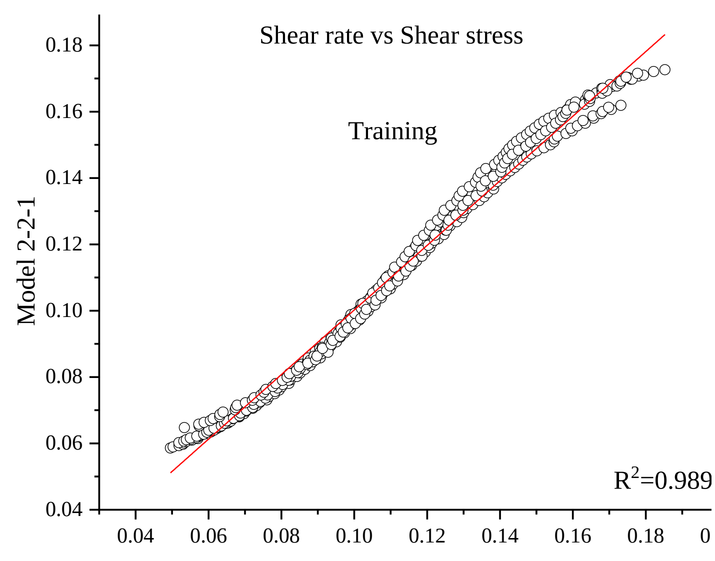

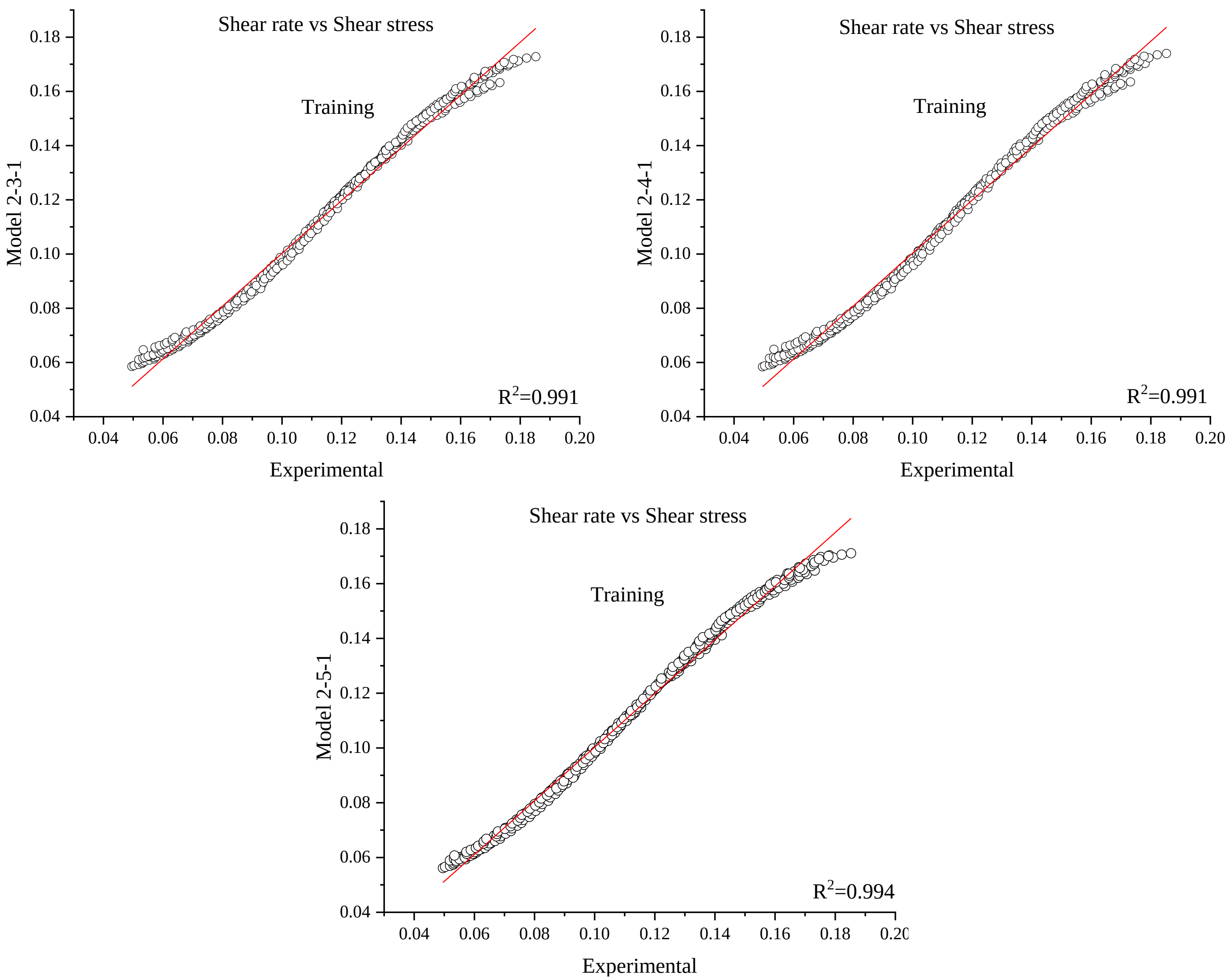

Figure 7. BPA 2 training results of shear stress obtained from each model

The testing of shear stress by BPA 2 is shown in Figure 8 using model 1 to 5. The testing of BPA 2 once the model is trained (as shown in Figure 7) indicates that the output is very close to experimental values. Though model 1 and 2 have not performed well in training the testing results indicate a good fit. However a model must be first proven in training to opt for testing of the data. The testing results indicate an R-squared value of 0.96. As there are lot of minor fluctuations in shear stress value with shear rate at some instance during the experiments the prediction by network need still huge data. The BPA 2 used for each model has shown almost a same nature of agreement due to lower number of points available. Increase in data may further help us in better prediction of the shear stress with respect to shear rate.

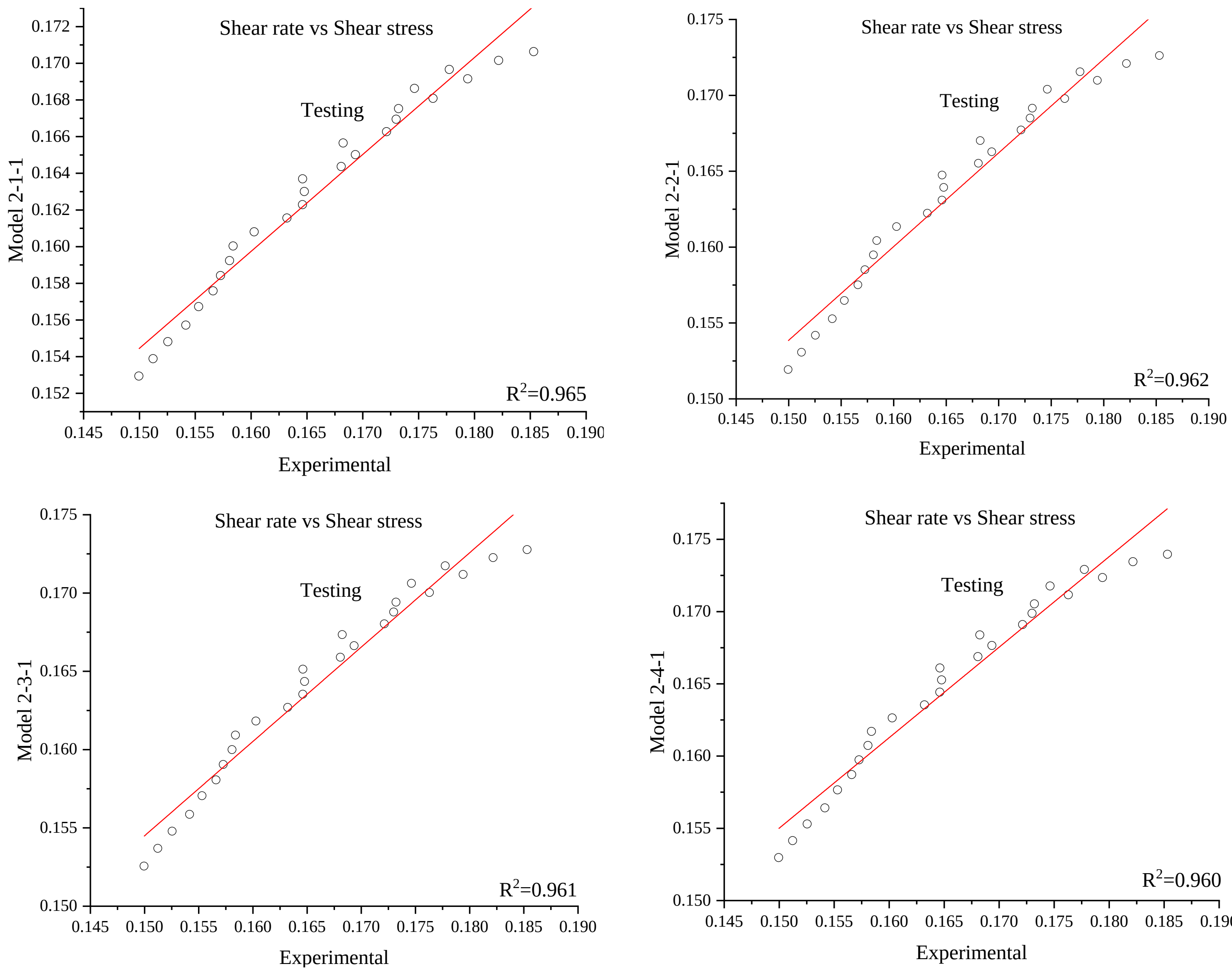

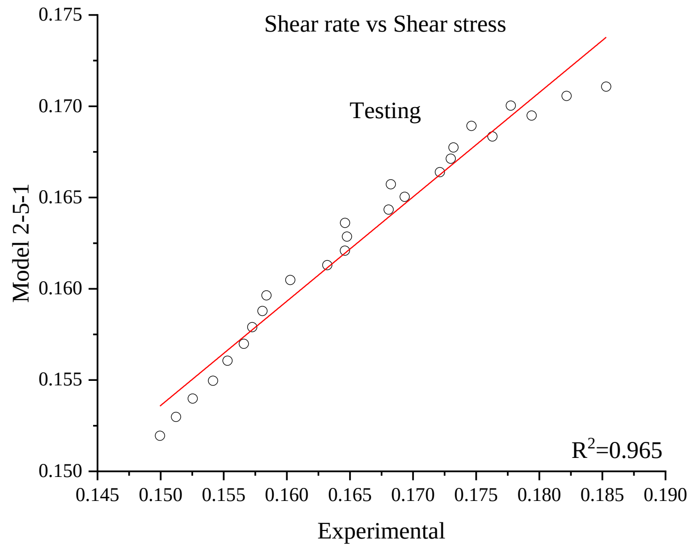

Figure 8. Testing of BPA 2 to predict shear stress

The BPA 3 used for regression of experimental data with viscosity as output and temperature and MXene nanoparticle wt. % in Ionic solution is shown in Figure 9. The data points are less in number which is around 200 and hence the successful training is an important task. With the model 2 to 5 the accuracy of the BPA 3 has remained same. Only model 1 shows larger deviations while for remaining models the R-squared value if 0.99 showing a good fit. However model 2 to 5 can be preferred as training is found to be successful. Here the shear rate is kept constant while temperature is increased from 20°C to 50°C. With the increase of temperature the viscosity has reduced which is non-linear. This non-linear data is found to be well predicted by the models. The improvement in the agreement between experimental and predicted data is so nicely inclining with the trendline can be easily made out. This is purely due to the increase of neurons in the hidden showing their greater impact on the efficiency of algorithm to predict the data.

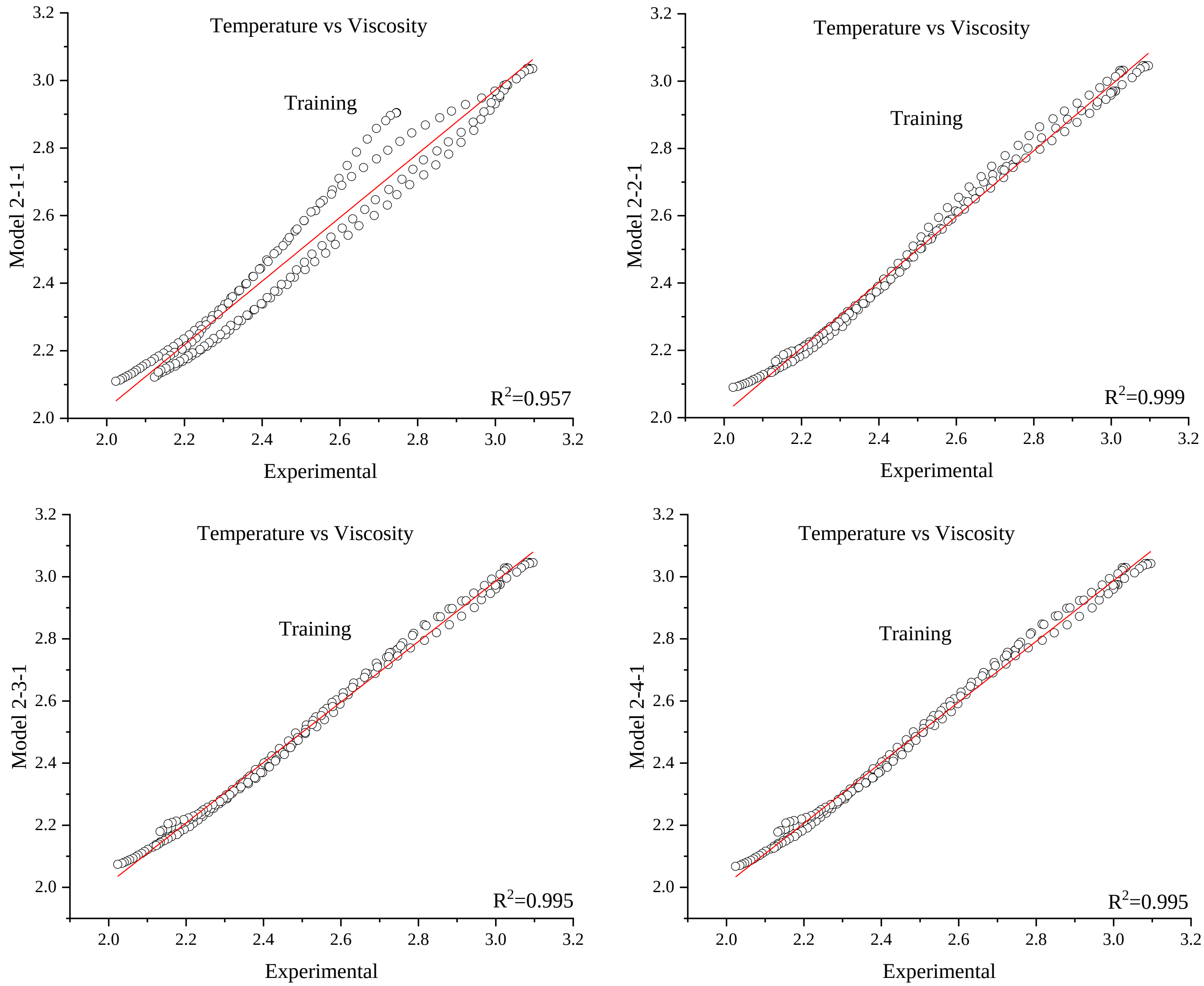
Temperature vs Viscosity
Training
Model 2-1-1
Experimental
R2=0.957
Temperature vs Viscosity
Training
Model 2-2-1
Experimental
R2=0.999
Temperature vs Viscosity
Training
Model 2-3-1
Experimental
R2=0.995
Temperature vs Viscosity
Training
Model 2-4-1
Experimental
R2=0.995

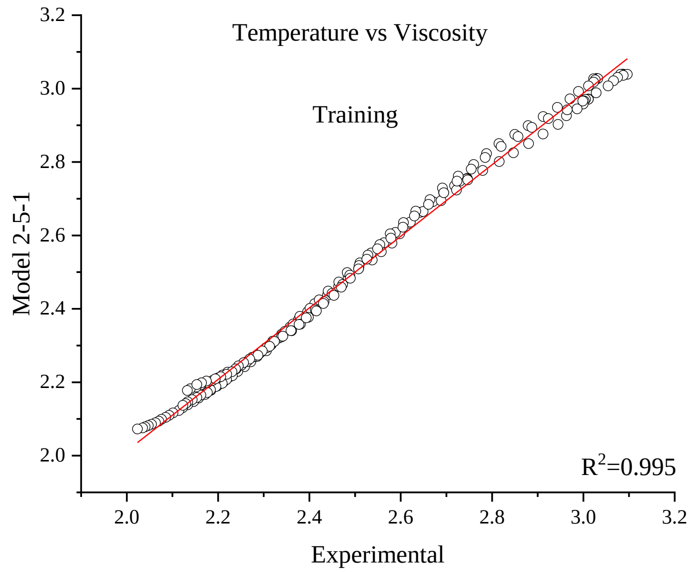

Figure 9. Training of BPA 3 to predict viscosity as a function of temperature and MXene nanoparticle wt. %

The testing of BPA 3 to predict the viscosity as a function of temperature is shown in Figure 10. The testing of BPA 3 shows that the viscosity predicted by each model is successful. The experimental viscosity and BPA 3 output during the testing is found to be well established. Based on the training of BPA 3 it can be inferred that models 2 to 5 are better suited for prediction though model 1 shows good agreement with the experimental values. The main reason for model 1 predicting the viscosity in testing is the low data points used. The last readings of viscosity were used which does not much change with temperature hence data with much fluctuations will indicate the proper fitness of the model 1.

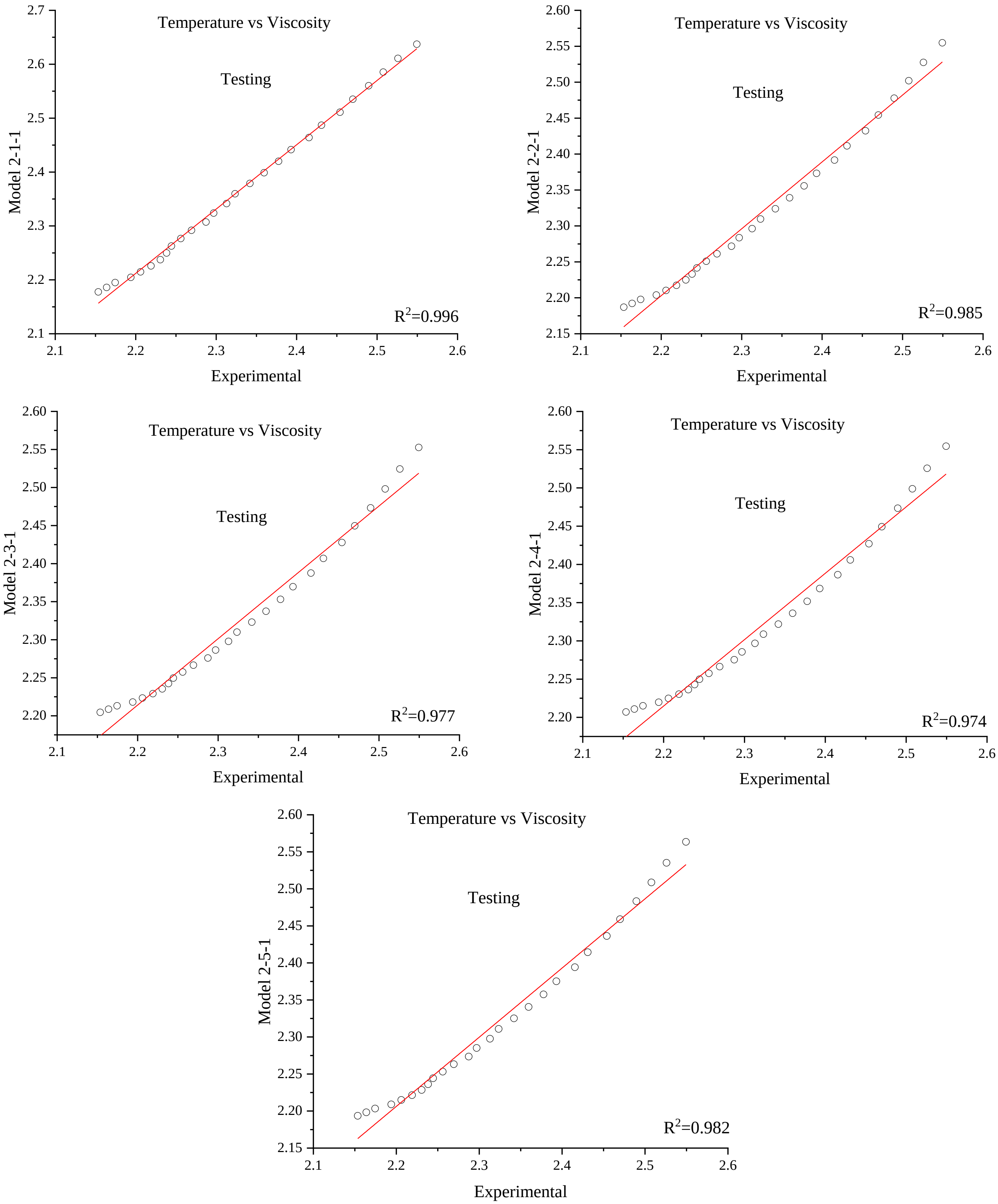

Figure 10. Testing of BPA 3 to predict viscosity

The BPA 4/5 used for modelling of viscosity and shear stress together are same. The training results of BPA 4 for viscosity is shown in Figure 11 (a). Here the fluctuations of viscosity prediction by model 1 is clearly noticed. Other models 2 to 5 are in the verge of exact prediction. However model 5 is closer than other. The inset figures provided clearly indicates this fact. When there are two outputs from a network, the weights and bias functions are completely different than the model having single output. But such a model is of more advantage than a single output network as the computational time is saved and robustness of model is increased. The testing of BPA 4 for viscosity is shown in Figure 11 (b). Again the testing of model 1 has shown large deviations. The other models have close values to experimental part. However to be consistent model 3 to model 5 are found to be robust in all algorithms adopted. The testing of model 2 to 5 have indicated a good agreement between the experimental part and BPA 4.

In Figure 12 the shear stress prediction using algorithm 5 is shown for 5 models. In line with the results provided by BPA 2 the predictions are similar. Model 1 and model 2 can be however neglected as also seen in previous case. The rest models 3 to 5 give comfortable agreement and fit between the experimental and network output. In Figure 13 the testing results obtained from BPA 5 is depicted for each model. It is seen that each model predicts comfortably the experimental test data points. All models have R-squared very close to unity. As mentioned in the preceding discussion the test results of model 1 cannot be considered as the training part is not found to be much accurate like other models. Hence as a general observation with the increase of number of neurons in hidden layer the model performance increases. But also it is seen that a certain maximum number of neurons in hidden layer are enough to accurately predict the output. If the neurons, as in this case are increased from 1 to 5, models 3 to 5 have shown very close results. Hence upper limit to number of neurons in hidden layer exists.

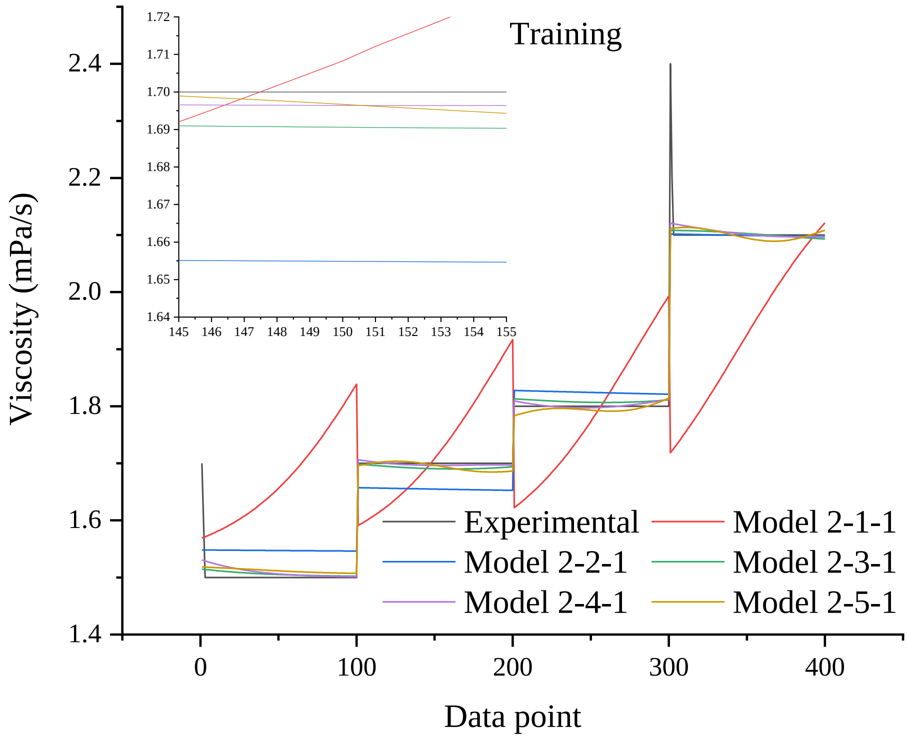

(a) Training of BPA 4 for viscosity

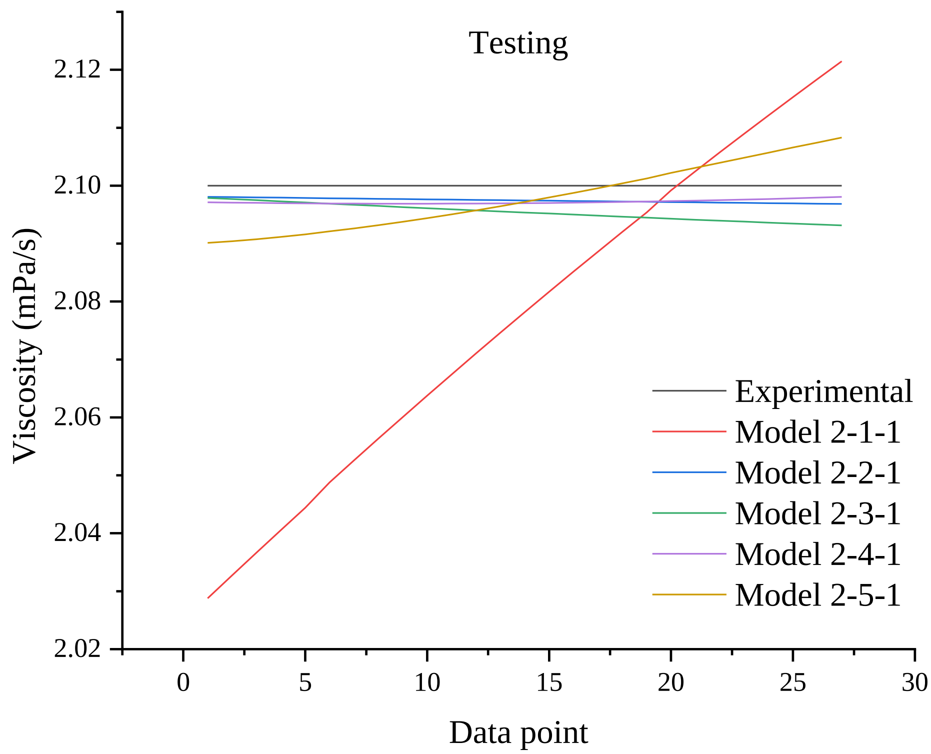

(b) Testing of BPA 4 for viscosity

Figure 11. BPA 4 training/testing results obtained for viscosity

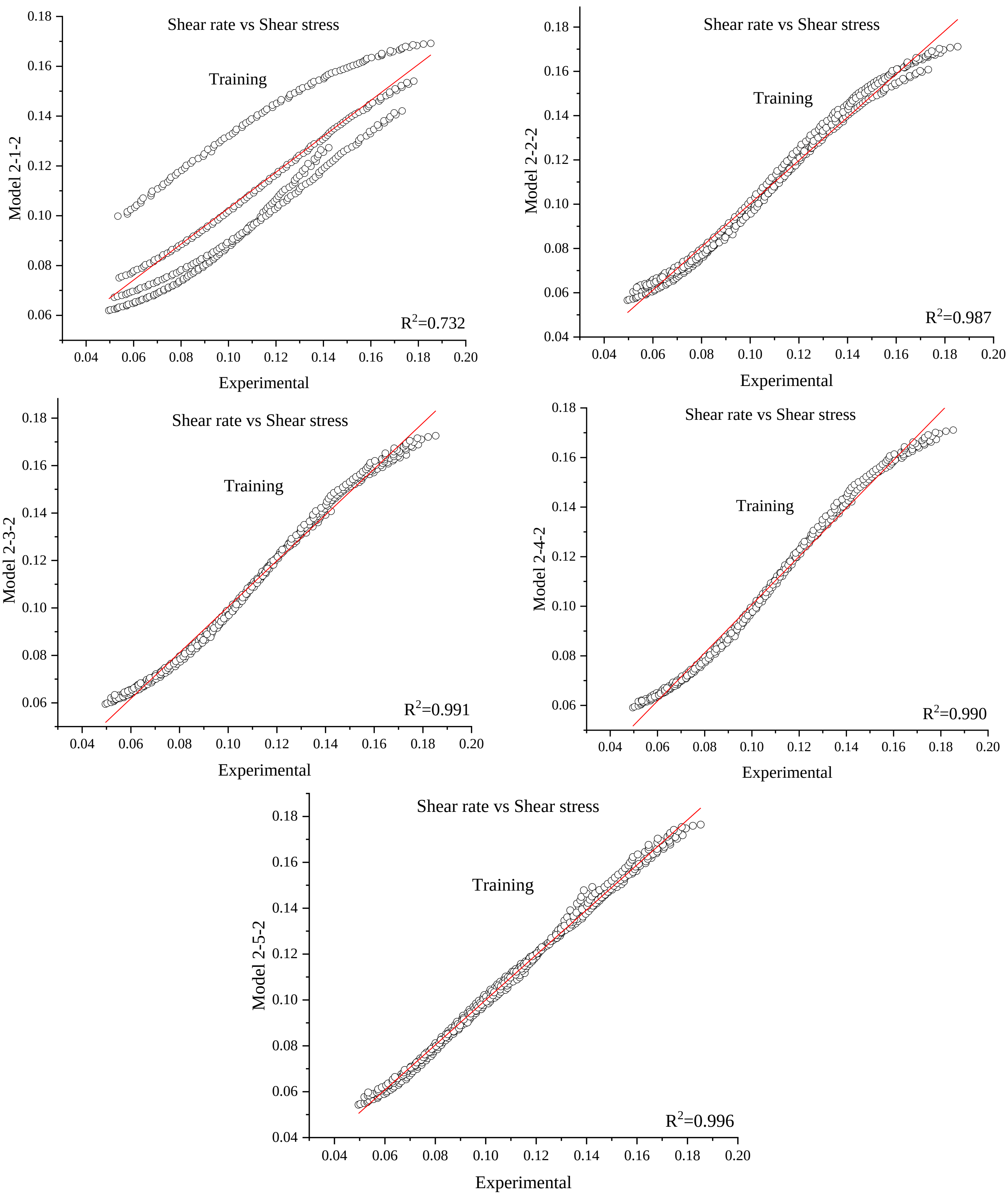

Figure 12. BPA 5 used for prediction of shear stress during the training process

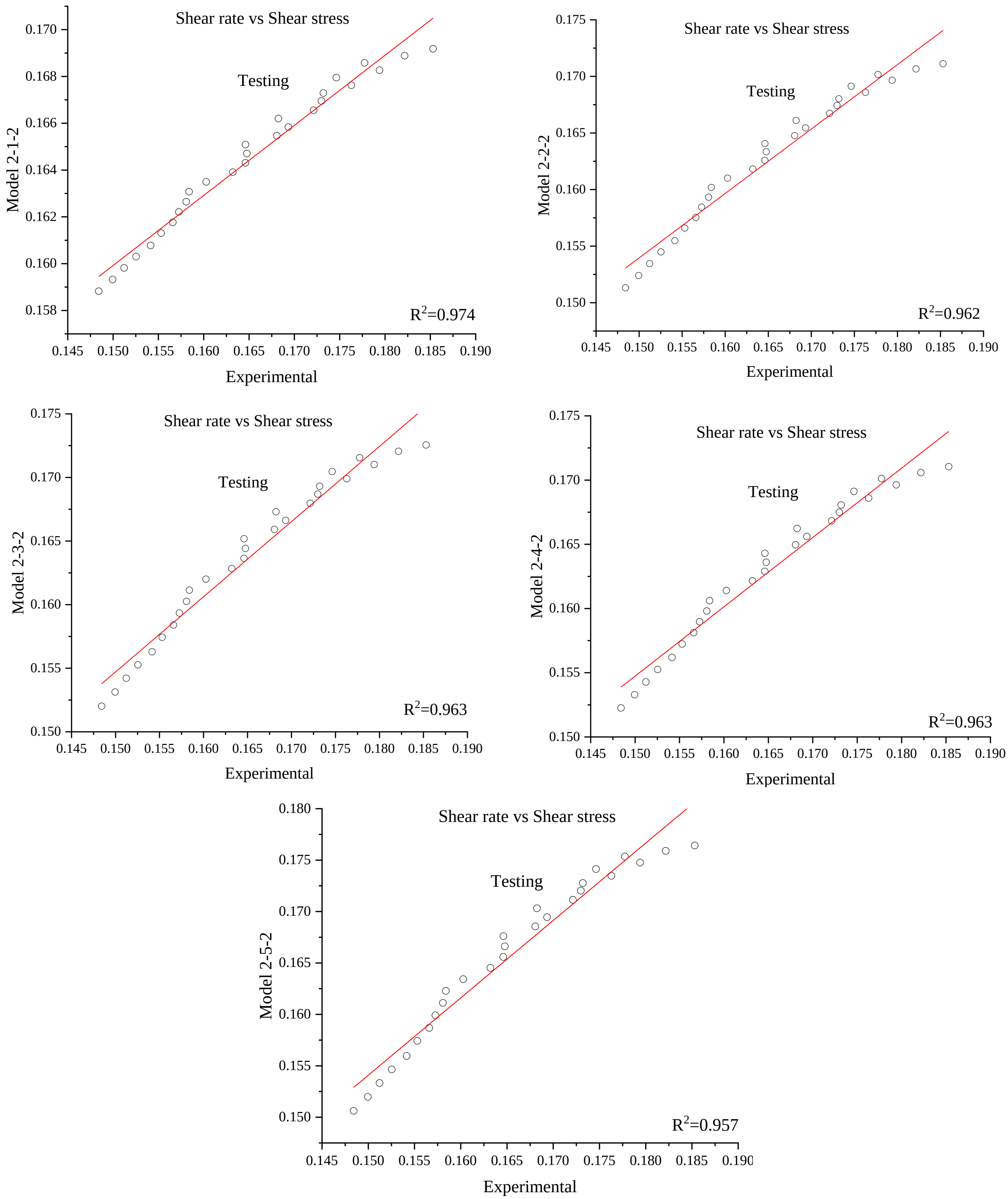

Figure 13. Testing of BPA 5 prediction of shear stress

Figure 14 (a) depicts validation results obtained from the NN modelling for BPA 2, 3 and 4 respectively for model 5 i.e. 5 neurons in hidden layer. It can be observed that Algorithm 2 to 4 validation results are very close to the experimental results. The data distribution for training, testing and validation is random and results shows the less deviations in case of validation process displaying a good fitness of model in prediction of output with considering the data which previously has been not used for training and testing. As mentioned earlier the algorithm 2 and 3 contains single output and 4 having two output and validation of these data is found to be effective. In case of model optimizing the neurons in hidden layer is essential. As seen in this study increasing the neuron in hidden layer gives the better performance. However, with limited neurons (<5) in hidden layer for prediction of data with multioutput has been responsible to provide effective results instead of having more neurons in hidden layer. Hence, upper limit of model 5 is considered for the presenting the validation results. In remaining models the observed validation results from the NN model is also close to experimental results but comparatively higher for the model 2 to 4 with algorithm 2, 3 and 4 respectively. The MSE obtained for these results are very close to zero (as seen in case of training and testing) and which gives proper validation of results. Similarly, the correlation coefficient of these algorithms I validation process has shown the value close to indicating the accuracy of viscosity and shear stress prediction.

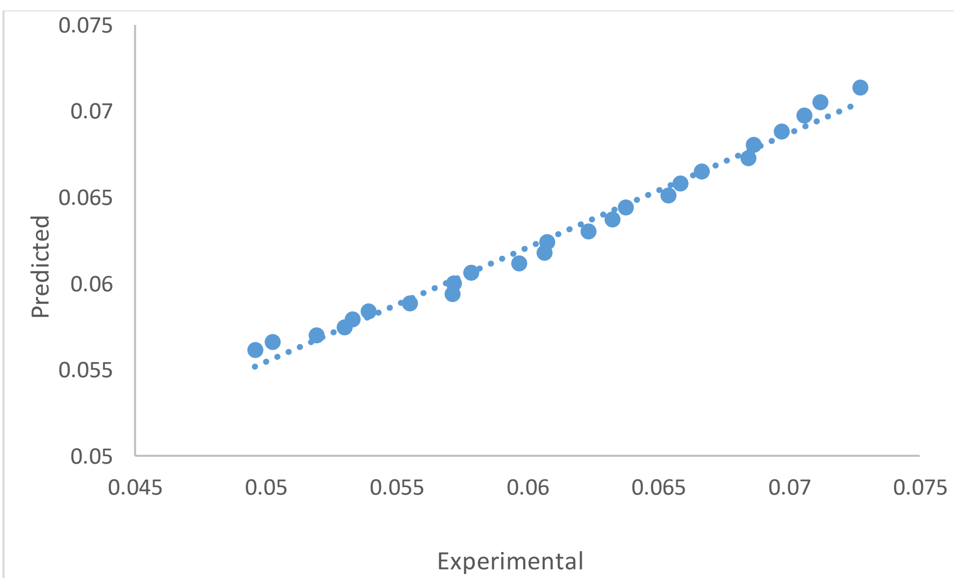

(a) Algorithm 2

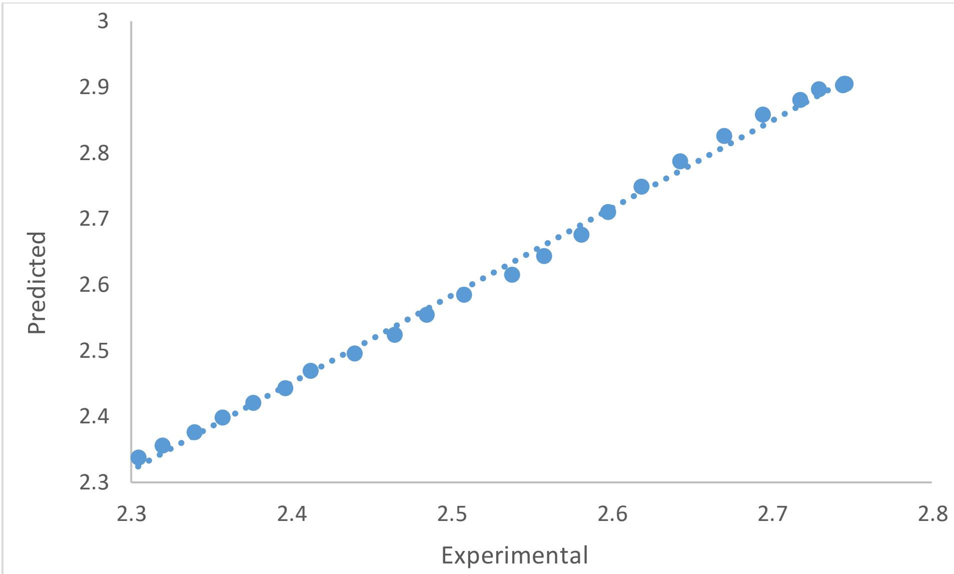

(b) Algorithm 3

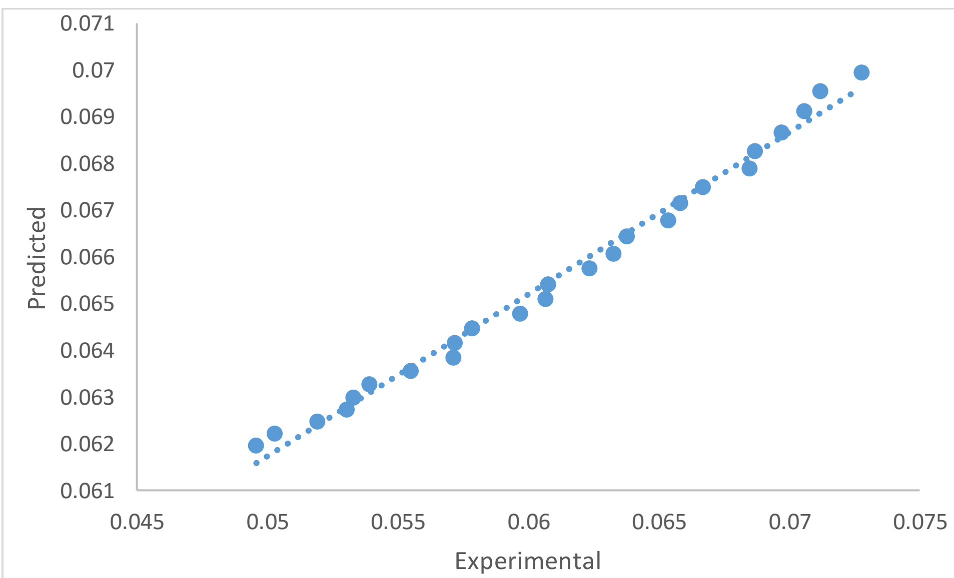

(c) Algorithm 4

Figure 14. Validation plots for algorithm 2-4

In Table 3 the weigth and bias values of Model 5 from BPA 1 is mentioned.

Table 3. Weight and Bias values of BPA 1 for Model 5

From the input layer

To the 1rst hidden layer	Bias	1th neuron	2th neuron	3th neuron	4th neuron
1th neuron	0.69301	0.007816	6.93545	-5.93534	5.417912
2th neuron	-5. 5181	0.0017742	0.51441	-11.4157	-26.95542
3th neuron	-21. 561	-0.0082714	-0.103354	-31.0137	1.137775
4th neuron	-2. 4624	-0.0071242	-2.78927	3.8025844	-0.101495
5th neuron	6. 9256	0.0080793	3.5414256=	12.902675	-0.707268

From the 1rst hidden layer

To the output layer	Bias	1th neuron	2th neuron	3th neuron	4th neuron	5th neuron
1th neuron	1.16612	4.84427	1.59697	8.37624	-6.08835	-12.0812

4. Conclusion

Back propagation modelling of the experimental data performed for the analysis of viscosity and shear stress of Ionic-MXene nanofluids of different wt. % is carried out in this article. Five back propagation algorithms (BPA) are developed for the modelling of data. In each BPA 5 models are developed to accurately predict the experimental data. It is found that the number of neurons in the hidden layer has a significant role in proper prediction. The training and testing of the developed algorithms is found to predict the shear stress and viscosity appropriately. The statistical analysis performed for the algorithms also reveal the good accuracy of the model. Model 1 having a single neuron is not able to predict the output giving a significant error. The viscosity and shear stress are predicted appropriately in the training and testing phase by each algorithm. The mean square error, root mean square error, error deviation %, and correlation coefficient for all the models in each BPA is analyzed. The statistical analysis reveals that all BPA are good for the prediction of viscosity and shear stress. However, Model 1 has much less accuracy than the remaining five models. In BPA 5 the accuracy of Model 1 further reduces as the input and output neurons increase. This has clearly indicated that the neurons in the hidden layer paly a significant role in viscosity and shear stress prediction. Further, the role of layers in between the input and output layer can be explored. Impact of random seed on accuracy of prediction and use of different activation functions needs to be explored as it is an interesting study.

References

[1] R. Saidur, K.Y. Leong, H.A. Mohammed, A review on applications and challenges of nanofluids, Renewable and Sustainable Energy Reviews. 15 (2011) 1646–1668. doi:10.1016/j.rser.2010.11.035.

[2] D. Dey, P. Kumar, S. Samantaray, A review of nanofluid preparation, stability, and thermo-physical properties, Heat Transfer - Asian Research. 46 (2017) 1413–1442. doi:10.1002/htj.21282.

[3] A.M. Hussein, K. Kadirgama, M.M. Noor, Nanoparticles suspended in ethylene glycol thermal properties and applications: An overview, Renewable and Sustainable Energy Reviews. 69 (2017) 1324–1330. doi:10.1016/j.rser.2016.12.047.

[4] A. Afzal, A.D.M. Samee, R.K.A. Razak, M.K. Ramis, Heat transfer characteristics of MWCNT nanofluid in rectangular mini channels, International Journal of Heat and Technology. 36 (2018) 222–228. doi:10.18280/ijht.360130.

[5] A. Afzal, A.R. Rk, M.S. Ad, M. Kareemulla, K.M. Yashwantha, S. Raju, E.H. Raghavendra, Heat Transfer Analysis of Triple Tube Heat Exchanger using Water and Titanium-dioxide Nanofluid, Twelve International Conference on Thermal Engineering: Theory and Applications. (2019) 1–3.

[6] V. Kumar, A.K. Tiwari, S.K. Ghosh, Application of nanofluids in plate heat exchanger: A review, Energy Conversion and Management. 105 (2015) 1017–1036. doi:10.1016/j.enconman.2015.08.053.

[7] P.K. Nagarajan, J. Subramani, S. Suyambazhahan, R. Sathyamurthy, Nanofluids for solar collector applications: A review, Energy Procedia. 61 (2014) 2416–2434. doi:10.1016/j.egypro.2014.12.017.

[8] S.K. Verma, A.K. Tiwari, Progress of nanofluid application in solar collectors: A review, Energy Conversion and Management. 100 (2015) 324–346. doi:10.1016/j.enconman.2015.04.071.

[9] O.A. Alawi, N.A.C. Sidik, A.S. Kherbeet, Nanorefrigerant effects in heat transfer

performance and energy consumption reduction: A review, International Communications in Heat and Mass Transfer. 69 (2015) 76–83. doi:10.1016/j.icheatmasstransfer.2015.10.009.

[10] A. Kasaeian, S.M. Hosseini, M. Sheikhpour, O. Mahian, W.M. Yan, S. Wongwises, Applications of eco-friendly refrigerants and nanorefrigerants: A review, Renewable and Sustainable Energy Reviews. 96 (2018) 91–99. doi:10.1016/j.rser.2018.07.033.

[11] M.A. Nazari, M.H. Ahmadi, M. Sadeghzadeh, M.B. Shafii, M. Goodarzi, A review on application of nanofluid in various types of heat pipes, Journal of Central South University. 26 (2019) 1021–1041. doi:10.1007/s11771-019-4068-9.

[12] R. Sureshkumar, S.T. Mohideen, N. Nethaji, Heat transfer characteristics of nanofluids in heat pipes: A review, Renewable and Sustainable Energy Reviews. 20 (2013) 397–410. doi:10.1016/j.rser.2012.11.044.

[13] J. Buongiorno, L.-W. Hu, S.J. Kim, R. Hannink, B. Truong, E. Forrest, Nanofluids for Enhanced Economics and Safety of Nuclear Reactors: An Evaluation of the Potential Features, Issues, and Research Gaps, Nuclear Technology. 162 (2008) 80–91. doi:10.13182/NT08-A3934.

[14] H.W. Xian, N.A.C. Sidik, G. Najafi, Recent state of nanofluid in automobile cooling systems, Journal of Thermal Analysis and Calorimetry. 135 (2019) 981–1008. doi:10.1007/s10973-018-7477-3.

[15] F. Ali, Aamina, I. Khan, N.A. Sheikh, M. Gohar, I. Tlili, Effects of Different Shaped Nanoparticles on the Performance of Engine-Oil and Kerosene-Oil: A generalized Brinkman-Type Fluid model with Non-Singular Kernel, Scientific Reports. 8 (2018) 1–13. doi:10.1038/s41598-018-33547-z.

[16] A. Ghadimi, I.H. Metselaar, The influence of surfactant and ultrasonic processing on improvement of stability, thermal conductivity and viscosity of titania nanofluid, Experimental Thermal and Fluid Science. 51 (2013) 1–9. doi:10.1016/j.expthermflusci.2013.06.001.

[17] F. Ali, L. Reinert, J. Levêque, L. Duclaux, F. Muller, S. Saeed, S. Sakhawat, Ultrasonics Sonochemistry Effect of sonication conditions : Solvent , time , temperature and reactor type on the preparation of micron sized vermiculite particles, ULTRASONICS SONOCHEMISTRY. (2013). doi:10.1016/j.ultsonch.2013.10.010.

[18] F. Li, L. Li, G. Zhong, Y. Zhai, Z. Li, Effects of ultrasonic time, size of aggregates and

temperature on the stability and viscosity of Cu-ethylene glycol (EG) nanofluids, International Journal of Heat and Mass Transfer. 129 (2019) 278–286. doi:10.1016/j.ijheatmasstransfer.2018.09.104.

[19] A. Asadi, I.M. Alarifi, V. Ali, H.M. Nguyen, An experimental investigation on the effects of ultrasonication time on stability and thermal conductivity of MWCNT-water nanofluid: Finding the optimum ultrasonication time, Ultrasonics Sonochemistry. 58 (2019) 104639. doi:10.1016/j.ultsonch.2019.104639.

[20] G. Xia, H. Jiang, R. Liu, Y. Zhai, Effects of surfactant on the stability and thermal conductivity of Al 2O3/de-ionized water nanofluids, International Journal of Thermal Sciences. 84 (2014) 118–124. doi:10.1016/j.ijthermalsci.2014.05.004.

[21] M.M. Tawfik, Experimental studies of nanofluid thermal conductivity enhancement and applications: A review, Renewable and Sustainable Energy Reviews. 75 (2017) 1239–1253. doi:10.1016/j.rser.2016.11.111.

[22] K.M. Yashawantha, A.V. Vinod, ANN modelling and experimental investigation on effective thermal conductivity of ethylene glycol : water nanofluids, Journal of Thermal Analysis and Calorimetry. (2020). doi:10.1007/s10973-020-09756-y.

[23] K.M. Yashawantha, A. Afzal, M.K. Ramis., J.U. Shareefraza, M.K. Ramis, S.J. Ukkund, Experimental investigation on physical and thermal properties of graphite nanofluids, in: AIP Conference Proceedings, 2018: p. 020057. doi:10.1063/1.5079016.

[24] K.M. Yashawantha, A. Asif, G. Ravindra Babu, M.K. Ramis, Rheological Behavior and Thermal Conductivity of Graphite–Ethylene Glycol Nanofluid, Journal of Testing and Evaluation. 49 (2021) Published ahead of print. doi:10.1520/JTE20190255.

[25] M. Hemmat Esfe, Designing an artificial neural network using radial basis function (RBF-ANN) to model thermal conductivity of ethylene glycol–water-based TiO2 nanofluids, Journal of Thermal Analysis and Calorimetry. 127 (2017) 2125–2131. doi:10.1007/s10973-016-5725-y.

[26] S.M. Vanaki, P. Ganesan, H.A. Mohammed, Numerical study of convective heat transfer of nanofluids: A review, Renewable and Sustainable Energy Reviews. 54 (2016) 1212–1239. doi:https://doi.org/10.1016/j.rser.2015.10.042.

[27] A.K. Tiwari, P. Ghosh, J. Sarkar, Heat transfer and pressure drop characteristics of CeO2/water nanofluid in plate heat exchanger, Applied Thermal Engineering. 57 (2013)

24–32. doi:10.1016/j.applthermaleng.2013.03.047.
[28] S.M.S. Murshed, P. Estellé, A state of the art review on viscosity of nanofluids, Renewable and Sustainable Energy Reviews. 76 (2017) 1134–1152. doi:10.1016/j.rser.2017.03.113.
[29] M. Ramezanizadeh, M.H. Ahmadi, M.A. Nazari, M. Sadeghzadeh, L. Chen, A review on the utilized machine learning approaches for modeling the dynamic viscosity of nanofluids, Renewable and Sustainable Energy Reviews. 114 (2019) 109345. doi:https://doi.org/10.1016/j.rser.2019.109345.
[30] M. Hemmat Esfe, M.R. Hassani Ahangar, M. Rejvani, D. Toghraie, M.H. Hajmohammad, Designing an artificial neural network to predict dynamic viscosity of aqueous nanofluid of TiO2 using experimental data, International Communications in Heat and Mass Transfer. 75 (2016) 192–196. doi:https://doi.org/10.1016/j.icheatmasstransfer.2016.04.002.
[31] M. Afrand, A. Ahmadi Nadooshan, M. Hassani, H. Yarmand, M. Dahari, Predicting the viscosity of multi-walled carbon nanotubes/water nanofluid by developing an optimal artificial neural network based on experimental data, International Communications in Heat and Mass Transfer. 77 (2016) 49–53. doi:https://doi.org/10.1016/j.icheatmasstransfer.2016.07.008.
[32] M. Vakili, S. Khosrojerdi, P. Aghajannezhad, M. Yahyaei, A hybrid artificial neural network-genetic algorithm modeling approach for viscosity estimation of graphene nanoplatelets nanofluid using experimental data, International Communications in Heat and Mass Transfer. 82 (2017) 40–48. doi:https://doi.org/10.1016/j.icheatmasstransfer.2017.02.003.
[33] M. Amani, P. Amani, A. Kasaeian, O. Mahian, I. Pop, S. Wongwises, Modeling and optimization of thermal conductivity and viscosity of MnFe2O4 nanofluid under magnetic field using an ANN, Scientific Reports. 7 (2017) 1–13. doi:10.1038/s41598-017-17444-5.
[34] N. Zhao, Z. Li, Experiment and Artificial Neural Network Prediction of Thermal Conductivity and Viscosity for Alumina-Water Nanofluids, Materials. 10 (2017) 552. doi:10.3390/ma10050552.
[35] F. Derakhshanfard, A. Mehralizadeh, Application of artificial neural networks for viscosity of crude oil-based nanofluids containing oxides nanoparticles, Journal of Petroleum Science and Engineering. 168 (2018) 263–272. doi:https://doi.org/10.1016/j.petrol.2018.05.018.
[36] M.S. Shadloo, A. Rahmat, A. Karimipour, S. Wongwises, Estimation of Pressure Drop of

Two-Phase Flow in Horizontal Long Pipes Using Artificial Neural Networks, Journal of Energy Resources Technology. 142 (2020). doi:10.1115/1.4047593.

[37] H.R. Ansari, M.J. Zarei, S. Sabbaghi, P. Keshavarz, A new comprehensive model for relative viscosity of various nanofluids using feed-forward back-propagation MLP neural networks, International Communications in Heat and Mass Transfer. 91 (2018) 158–164. doi:10.1016/j.icheatmasstransfer.2017.12.012.

[38] M.H. Ahmadi, B. Mohseni-Gharyehsafa, M. Farzaneh-Gord, R.D. Jilte, R. Kumar, K. wing Chau, Applicability of connectionist methods to predict dynamic viscosity of silver/water nanofluid by using ANN-MLP, MARS and MPR algorithms, Engineering Applications of Computational Fluid Mechanics. 13 (2019) 220–228. doi:10.1080/19942060.2019.1571442.

[39] B. Anil Kumar Naik, A. Venu Vinod, ANN Modeling of the Viscosity and Effective Thermal Conductivity of Non-Newtonian Nanofluids, Journal of Testing and Evaluation. 47 (2019) 791–808. doi:10.1520/JTE20170274.

[40] A. Shahsavar, S. Khanmohammadi, D. Toghraie, H. Salihepour, Experimental investigation and develop ANNs by introducing the suitable architectures and training algorithms supported by sensitivity analysis: Measure thermal conductivity and viscosity for liquid paraffin based nanofluid containing Al2O3 nanoparticles, Journal of Molecular Liquids. 276 (2019) 850–860. doi:https://doi.org/10.1016/j.molliq.2018.12.055.

[41] M.H. Ahmadi, M. Sadeghzadeh, H. Maddah, A. Solouk, R. Kumar, K. wing Chau, Precise smart model for estimating dynamic viscosity of SiO2/ethylene glycol–water nanofluid, Engineering Applications of Computational Fluid Mechanics. 13 (2019) 1095–1105. doi:10.1080/19942060.2019.1668303.

[42] D. Toghraie, N. Sina, N.A. Jolfaei, M. Hajian, M. Afrand, Designing an Artificial Neural Network (ANN) to predict the viscosity of Silver/Ethylene glycol nanofluid at different temperatures and volume fraction of nanoparticles, Physica A: Statistical Mechanics and Its Applications. 534 (2019) 122142. doi:https://doi.org/10.1016/j.physa.2019.122142.

[43] D. Yadav, P. Dansena, S.K. Ghosh, P.K. Singh, A unique multilayer perceptron model (ANN) for different oxide/EG nanofluid's viscosity from the experimental study, Physica A: Statistical Mechanics and Its Applications. 549 (2020) 124030. doi:10.1016/j.physa.2019.124030.

[44] N. Parashar, M. Seraj, S. Mohd, Y. Mohd, Development of an artificial neural network for the prediction of relative viscosity of ethylene glycol based nanofluids, SN Applied Sciences. (2020). doi:10.1007/s42452-020-03269-x.

[45] I.O. Alade, M.A.A. Rahman, A. Hassan, T.A. Saleh, Modeling the viscosity of nanofluids using artificial neural network and Bayesian support vector regression, Journal of Applied Physics. 128 (2020) 085306(1–13). doi:10.1063/5.0008977.

[46] N. Parashar, N. Aslfattahi, S.M. Yahya, R. Saidur, An artificial neural network approach for the prediction of dynamic viscosity of MXene-palm oil nanofluid using experimental data, Journal of Thermal Analysis and Calorimetry. (2020). doi:10.1007/s10973-020-09638-3.

[47] L. Das, K. Habib, R. Saidur, N. Aslfattahi, S.M. Yahya, F. Rubbi, Improved thermophysical properties and energy efficiency of aqueous ionic liquid/mxene nanofluid in a hybrid pv/t solar system, Nanomaterials. 10 (2020) 1–26. doi:10.3390/nano10071372.

[48] R.B. Lopes N, Hybrid Learning in a Multi Neural Network Architecture, in: IEEE International Joint Conference on Neural Networks, 2001: pp. 2788–2793.

[49] N. Lopes, B. Ribeiro, GPU implementation of the multiple back-propagation algorithm, Lecture Notes in Computer Science (Including Subseries Lecture Notes in Artificial Intelligence and Lecture Notes in Bioinformatics). 5788 LNCS (2009) 449–456. doi:10.1007/978-3-642-04394-9_55.

[50] N. Lopes, B. Ribeiro, Stochastic GPU-based multithread implementation of multiple back-propagation, ICAART 2010 - 2nd International Conference on Agents and Artificial Intelligence, Proceedings. 1 (2010) 271–276. doi:10.5220/0002722102710276.

[51] N. Lopes, B. Ribeiro, An evaluation of multiple feed-forward networks on GPUs, International Journal of Neural Systems. 21 (2011) 31–47. doi:10.1142/S0129065711002638.